Physics Faculty Publications   Physics Department

1-1-2008

Electroexcitation of the Roper resonance for 1.7

I. G. Aznauryan

Angela Biselli
Fairfield University, abiselli@fairfield.edu

CLAS Collaboration

Peer Reviewed

Electroexcitation of the Roper resonance for $1.7 < Q^2 < 4.5\,\mathrm{GeV}^2$ in $\vec{e}\,p \to en\pi^+$

I. G. Aznauryan,[1,2] V. D. Burkert,[1] W. Kim,[4] K. Park,[3,4] G. Adams,[36] M. J. Amaryan,[34] P. Ambrozewicz,[18] M. Anghinolfi,[24]
G. Asryan,[2] H. Avakian,[1] H. Bagdasaryan,[2,34] N. Baillie,[43] J. P. Ball,[6] N. A. Baltzell,[3] S. Barrow,[19] V. Batourine,[4]
M. Battaglieri,[24] I. Bedlinskiy,[26] M. Bektasoglu,[34] M. Bellis,[9] N. Benmouna,[20] B. L. Berman,[20] A. S. Biselli,[9,17,36]
L. Blaszczyk,[19] B. E. Bonner,[37] C. Bookwalter,[19] S. Bouchigny,[25] S. Boiarinov,[1,26] R. Bradford,[9] D. Branford,[15]
W. J. Briscoe,[20] W. K. Brooks,[1,14] S. Bültmann,[34] C. Butuceanu,[43] J. R. Calarco,[31] S. L. Careccia,[34] D. S. Carman,[1] L. Casey,[10]
A. Cazes,[3] S. Chen,[19] L. Cheng,[10] P. L. Cole,[1,10,22] P. Collins,[6] P. Coltharp,[19] D. Cords,[1,*] P. Corvisiero,[24] D. Crabb,[42]
V. Crede,[19] J. P. Cummings,[36] D. Dale,[22] N. Dashyan,[2] R. De Masi,[11,25] R. De Vita,[24] E. De Sanctis,[23] P. V. Degtyarenko,[1]
H. Denizli,[35] L. Dennis,[19] A. Deur,[1] S. Dhamija,[18] K. V. Dharmawardane,[34] K. S. Dhuga,[20] R. Dickson,[9] C. Djalali,[3]
G. E. Dodge,[34] J. Donnelly,[21] D. Doughty,[1,12] M. Dugger,[6] M. Dugger,[35] O. P. Dzyubak,[3] H. Egiyan,[1,31] K. S. Egiyan,[2,*]
L. El Fassi,[5] L. Elouadrhiri,[1] P. Eugenio,[9,19] R. Fatemi,[42] G. Fedotov,[30] G. Feldman,[20] R. J. Feuerbach,[9] T. A. Forest,[22,34]
A. Fradi,[25] H. Funsten,[43,*] M. Y. Gabrielyan,[18] M. Garçon,[11] G. Gavalian,[31,34] N. Gevorgyan,[2] G. P. Gilfoyle,[38]
K. L. Giovanetti,[27] F. X. Girod,[1,11] J. T. Goetz,[7] W. Gohn,[13] E. Golovatch,[24,30] A. Gonenc,[18] C. I. O. Gordon,[21] R. W. Gothe,[3]
L. Graham,[3] K. A. Griffioen,[43] M. Guidal,[25] M. Guillo,[3] N. Guler,[34] L. Guo,[1] V. Gyurjyan,[1] C. Hadjidakis,[25] K. Hafidi,[5]
K. Hafnaoui,[5] H. Hakobyan,[2] R. S. Hakobyan,[10] C. Hanretty,[19] J. Hardie,[1,12] N. Hassall,[21] D. Heddle,[1] F. W. Hersman,[31]
K. Hicks,[33] I. Hleiqawi,[33] M. Holtrop,[31] C. E. Hyde,[34] Y. Ilieva,[3,20] D. G. Ireland,[21] B. S. Ishkhanov,[30] E. L. Isupov,[30]
M. M. Ito,[1] D. Jenkins,[41] H. S. Jo,[25] J. R. Johnstone,[21] K. Joo,[13,42] H. G. Juengst,[20,34] N. Kalantarians,[34] D. Keller,[33]
J. D. Kellie,[21] M. Khandaker,[32] K. Y. Kim,[35] A. Klein,[34] F. J. Klein,[10,18] A. V. Klimenko,[34] M. Kossov,[26] Z. Krahn,[9]
L. H. Kramer,[1,18] V. Kubarovsky,[1,36] J. Kuhn,[9,36] S. E. Kuhn,[34] S. V. Kuleshov,[26] V. Kuznetsov,[4] J. Lachniet,[9,34] J. M. Laget,[1,11]
J. Langheinrich,[3] D. Lawrence,[29] T. Lee,[31] Ji Li,[36] A. C. S. Lima,[20] K. Livingston,[21] H. Y. Lu,[3] K. Lukashin,[10]
M. MacCormick,[25] N. Markov,[13] P. Mattione,[37] S. McAleer,[19] B. McKinnon,[21] J. W. C. McNabb,[9] B. A. Mecking,[1]
S. Mehrabyan,[35] J. J. Melone,[21] M. D. Mestayer,[1] C. A. Meyer,[9] T. Mibe,[33] K. Mikhailov,[26] R. Minehart,[42] M. Mirazita,[23]
R. Miskimen,[29] V. Mokeev,[1,30] L. Morand,[11] B. Moreno,[25] K. Moriya,[9] S. A. Morrow,[11,25] M. Moteabbed,[18] J. Mueller,[35]
E. Munevar,[20] G. S. Mutchler,[37] P. Nadel-Turonski,[20] R. Nasseripour,[3,20] S. Niccolai,[20,25] G. Niculescu,[27,33] I. Niculescu,[1,20,27]
B. B. Niczyporuk,[1] M. R. Niroula,[34] R. A. Niyazov,[1,34] M. Nozar,[1,39] G. V. O'Rielly,[20] M. Osipenko,[24] A. I. Ostrovidov,[19]
S. Park,[19] E. Pasyuk,[6] C. Paterson,[21] S. Anefalos Pereira,[23] S. A. Philips,[20] J. Pierce,[42] N. Pivnyuk,[26] D. Pocanic,[42]
O. Pogorelko,[26] E. Polli,[23] I. Popa,[20] S. Pozdniakov,[26] B. M. Preedom,[3] J. W. Price,[8] Y. Prok,[1,12,28] D. Protopopescu,[21,31]
L. M. Qin,[34] B. A. Raue,[1,18] G. Riccardi,[19] G. Ricco,[24] M. Ripani,[24] B. G. Ritchie,[6] G. Rosner,[21] P. Rossi,[23] D. Rowntree,[28]
P. D. Rubin,[38] F. Sabatié,[11,34] M. S. Saini,[19] J. Salamanca,[22] C. Salgado,[32] J. P. Santoro,[1,10] V. Sapunenko,[1,24] D. Schott,[18]
R. A. Schumacher,[9] V. S. Serov,[26] Y. G. Sharabian,[1] D. Sharov,[30] J. Shaw,[29] N. V. Shvedunov,[30] A. V. Skabelin,[28] E. S. Smith,[1]
L. C. Smith,[42] D. I. Sober,[10] D. Sokhan,[15] A. Stavinsky,[26] S. S. Stepanyan,[4] S. Stepanyan,[1] B. E. Stokes,[19] P. Stoler,[36]
I. I. Strakovsky,[20] S. Strauch,[3] R. Suleiman,[28] M. Taiuti,[24] T. Takeuchi,[19] D. J. Tedeschi,[3,16] A. Tkabladze,[20,33] S. Tkachenko,[34]
L. Todor,[9,38] C. Tur,[3] M. Ungaro,[13,36] M. F. Vineyard,[38,40] A. V. Vlassov,[26] D. P. Watts,[15,21] L. B. Weinstein,[34] D. P. Weygand,[1]
M. Williams,[9] E. Wolin,[1] M. H. Wood,[3,29] A. Yegneswaran,[1] J. Yun,[34] M. Yurov,[4] L. Zana,[31] B. Zhang,[28] J. Zhang,[34]
B. Zhao,[13] and Z. W. Zhao[3]

(CLAS Collaboration)

[1]*Thomas Jefferson National Accelerator Facility, Newport News, Virginia 23606, USA*
[2]*Yerevan Physics Institute, 375036 Yerevan, Armenia*
[3]*University of South Carolina, Columbia, South Carolina 29208, USA*
[4]*Kyungpook National University, Daegu 702-701, Republic of Korea*
[5]*Argonne National Laboratory, Argonne, Illinois 60439, USA*
[6]*Arizona State University, Tempe, Arizona 85287-1504, USA*
[7]*University of California at Los Angeles, Los Angeles, California 90095-1547, USA*
[8]*California State University, Dominguez Hills, Carson, California 90747, USA*
[9]*Carnegie Mellon University, Pittsburgh, Pennsylvania 15213, USA*
[10]*Catholic University of America, Washington, D.C. 20064, USA*
[11]*CEA-Saclay, Service de Physique Nucléaire, F-91191 Gif-sur-Yvette, France*
[12]*Christopher Newport University, Newport News, Virginia 23606, USA*
[13]*University of Connecticut, Storrs, Connecticut 06269, USA*
[14]*Universidad Técnica Federico Santa María, Casilla 110-V, Valparaíso, Chile*
[15]*Edinburgh University, Edinburgh EH9 3JZ, United Kingdom*
[16]*Emmy-Noether Foundation, Germany*
[17]*Fairfield University, Fairfield, Connecticut 06824, USA*
[18]*Florida International University, Miami, Florida 33199, USA*
[19]*Florida State University, Tallahassee, Florida 32306, USA*
[20]*The George Washington University, Washington, D.C. 20052, USA*
[21]*University of Glasgow, Glasgow G12 8QQ, United Kingdom*

^{22}*Idaho State University, Pocatello, Idaho 83209, USA*
^{23}*INFN, Laboratori Nazionali di Frascati, I-00044 Frascati, Italy*
^{24}*INFN, Sezione di Genova, I-16146 Genova, Italy*
^{25}*Institut de Physique Nucleaire ORSAY, Orsay, France*
^{26}*Institute of Theoretical and Experimental Physics, Moscow, RU-117259, Russia*
^{27}*James Madison University, Harrisonburg, Virginia 22807, USA*
^{28}*Massachusetts Institute of Technology, Cambridge, Massachusetts 02139-4307, USA*
^{29}*University of Massachusetts, Amherst, Massachusetts 01003, USA*
^{30}*Moscow State University, General Nuclear Physics Institute, RU-119899 Moscow, Russia*
^{31}*University of New Hampshire, Durham, New Hampshire 03824-3568, USA*
^{32}*Norfolk State University, Norfolk, Virginia 23504, USA*
^{33}*Ohio University, Athens, Ohio 45701, USA*
^{34}*Old Dominion University, Norfolk, Virginia 23529, USA*
^{35}*University of Pittsburgh, Pittsburgh, Pennsylvania 15260, USA*
^{36}*Rensselaer Polytechnic Institute, Troy, New York 12180-3590, USA*
^{37}*Rice University, Houston, Texas 77005-1892, USA*
^{38}*University of Richmond, Richmond, Virginia 23173, USA*
^{39}*TRIUMF, 4004, Wesbrook Mall, Vancouver, British Columbia V6T 2A3, Canada*
^{40}*Union College, Schenectady, New York 12308, USA*
^{41}*Virginia Polytechnic Institute and State University, Blacksburg, Virginia 24061-0435, USA*
^{42}*University of Virginia, Charlottesville, Virginia 22901, USA*
^{43}*College of William and Mary, Williamsburg, Virginia 23187-8795, USA*

The helicity amplitudes of the electroexcitation of the Roper resonance are extracted for $1.7 < Q^2 < 4.5\,\text{GeV}^2$ from recent high precision JLab-CLAS cross section and longitudinally polarized beam asymmetry data for π^+ electroproduction on protons at $W = 1.15 - 1.69$ GeV. The analysis is made using two approaches, dispersion relations and a unitary isobar model, which give consistent Q^2 behavior of the helicity amplitudes for the $\gamma^* p \to \text{N}(1440)\text{P}_{11}$ transition. It is found that the transverse helicity amplitude $A_{1/2}$, which is large and negative at $Q^2 = 0$, becomes large and positive at $Q^2 \simeq 2\,\text{GeV}^2$, and then drops slowly with Q^2. The longitudinal helicity amplitude $S_{1/2}$, which was previously found from CLAS $\vec{e}p \to ep\pi^0, en\pi^+$ data to be large and positive at $Q^2 = 0.4, 0.65\,\text{GeV}^2$, drops with Q^2. Available model predictions for $\gamma^* p \to \text{N}(1440)\text{P}_{11}$ allow us to conclude that these results provide strong evidence in favor of N(1440)P$_{11}$ as a first radial excitation of the $3q$ ground state. The results of the present paper also confirm the conclusion of our previous analysis for $Q^2 < 1$ GeV^2 that the presentation of N(1440)P$_{11}$ as a q^{3}G hybrid state is ruled out.

DOI: 10.1103/PhysRevC.78.045209   PACS number(s): 13.60.Le, 11.55.Fv, 13.40.Gp, 14.20.Gk

The excitation of nucleon resonances in electromagnetic interactions has long been recognized as a sensitive source of information on the long- and short-range structure of the nucleon and its excited states in the domain of quark confinement. Constituent quark models (CQM) have been developed that relate electromagnetic resonance transition form factors to fundamental quantities, such as the quark confining potential. While this relationship is more direct for heavy quarks, even in the light quark sector such connections exist and may be probed by measuring transition form factors over a large range in photon virtuality Q^2, which defines the space-time resolution of the probe.

The so-called Roper resonance, or N(1440)P$_{11}$, is the lowest excited state of the nucleon. In the CQM, the simplest and most natural assumption is that this is the first radial excitation of the $3q$ ground state. However, calculations within the nonrelativistic CQM fail to reproduce even the sign of

the transition photocoupling amplitude [1]. Moreover, the mass of the state is more than 100 MeV lower than what is predicted in the CQM with gluon exchange interaction [2,3]. More recent models that include also Goldstone boson exchange between quarks gave better agreement with the mass [4]. To deal with shortcomings of the quark model, alternative descriptions of N(1440)P$_{11}$ were developed, where this resonance is treated respectively as: a hybrid q^3G state where the three quarks are bound together with a gluon [5,6], a quark core dressed by a meson cloud [7,8], and a dynamically generated πN resonance [9]; other models include $3q - q\bar{q}$ components, in particular a strong σN component (see Ref. [10] and references therein). Discrimination between these descriptions of the Roper resonance can provide deep insight into the underlying basic symmetries and the structure of quark confinement.

The Q^2 dependence of the electromagnetic transition form factors is highly sensitive to different descriptions of the Roper state. However, until recently, the data base used to extract these form factors was almost exclusively based on π^0

---

*Deceased.

production, and very limited in kinematical coverage. Also, the $\pi^0 p$ final state is dominated by the nearby isospin $\frac{3}{2}$ $\Delta(1232)P_{33}$ resonance, whereas the isospin $\frac{1}{2}$ Roper state couples more strongly to the $\pi^+ n$ channel. The CLAS Collaboration has now published a large body of precise differential cross sections and polarized beam asymmetries for the process $\vec{e}p \rightarrow en\pi^+$ in the range of invariant hadronic mass $W = 1.15 - 1.69$ GeV and photon virtuality $Q^2 = 1.7 - 4.5$ GeV^2, with full azimuthal and polar angle coverage [11]. In this paper we report the results on the electroexcitation of the Roper resonance extracted from this large data set.

The approaches we use to analyze the data—fixed-t dispersion relations (DR) and a unitary isobar model (UIM)—were described in detail in Refs. [12,13] and were successfully employed in Refs. [12–14] for analyses of pion-photoproduction and low-Q^2-electroproduction data. The UIM of Refs. [12,13] was developed on the basis of MAID (Ref. [15]); the main modification consisted in the incorporation of Regge poles with increasing energies. The analysis of the data for $Q^2 = 1.7 - 4.5$ GeV^2 showed that for the best description of the data for these Q^2, Regge poles should be included at higher energies than those which we investigate in this analysis; therefore, the UIM we use for $Q^2 = 1.7 - 4.5$ GeV^2 is very close to MAID [15,16].

We have taken into account all resonances from the first, second, and third resonance regions. These are four- and three-star resonances $\Delta(1232)P_{33}$, $N(1440)P_{11}$, $N(1520)D_{13}$, $N(1535)S_{11}$, $\Delta(1600)P_{33}$, $\Delta(1620)S_{31}$, $N(1650)S_{11}$, $N(1675)D_{15}$, $N(1680)F_{15}$, $N(1700)D_{13}$, $\Delta(1700)D_{33}$, $N(1710)P_{11}$, and $N(1720)P_{13}$. For the masses, widths, and πN branching ratios of these resonances, we used the mean values of the data presented in the Review of Particle Physics (RPP) [17]. In particular for the Roper resonance, the values $M = 1.44$ GeV, $\Gamma = 0.35$ GeV, and $\beta_{\pi N} = 0.6$ were taken. Resonances of the fourth resonance region practically have no influence in the energy region under investigation and were not included.

The fitting parameters in our analysis were the $\gamma^* p \rightarrow N^{*+}$ helicity amplitudes, $A_{1/2}$, $A_{3/2}$, $S_{1/2}$, which are related to the resonance contributions to the multipole amplitudes at the resonance positions in the following way [1,17–19]:

$$Im M_{l\pm}(E_{l\pm}, S_{l\pm})(W = M) \equiv a\mathcal{M}_{l\pm}(\mathcal{E}_{l\pm}, \mathcal{S}_{l\pm}), \quad (1)$$

$$a \equiv C_I \left[\frac{1}{(2J+1)\pi} \frac{k_r}{q_r} \frac{m}{M} \frac{\beta_{\pi N}}{\Gamma} \right]^{1/2}, \quad (2)$$

$$C_{1/2} = -\sqrt{\frac{1}{3}}, \quad C_{3/2} = \sqrt{\frac{2}{3}} \text{ for } \gamma^* p \rightarrow \pi^0 p, \quad (3)$$

$$C_{1/2} = -\sqrt{\frac{2}{3}}, \quad C_{3/2} = -\sqrt{\frac{1}{3}} \text{ for } \gamma^* p \rightarrow \pi^+ n, \quad (4)$$

$$A_{1/2}^{l+} = -\frac{1}{2}[(l+2)\mathcal{E}_{l+} + l\mathcal{M}_{l+}], \quad (5)$$

$$A_{3/2}^{l+} = \frac{[l(l+2)]^{1/2}}{2}(\mathcal{E}_{l+} - \mathcal{M}_{l+}), \quad (6)$$

$$S_{1/2}^{l+} = -\frac{1}{\sqrt{2}}(l+1)\mathcal{S}_{l+}, \quad (7)$$

$$A_{1/2}^{(l+1)-} = \frac{1}{2}\left[(l+2)\mathcal{M}_{(l+1)-} - l\mathcal{E}_{(l+1)-}\right], \quad (8)$$

$$A_{3/2}^{(l+1)-} = -\frac{[l(l+2)]^{1/2}}{2}(\mathcal{E}_{(l+1)-} + \mathcal{M}_{(l+1)-}), \quad (9)$$

$$S_{1/2}^{(l+1)-} = -\frac{1}{\sqrt{2}}(l+1)\mathcal{S}_{(l+1)-}. \quad (10)$$

In Eq. (2), Γ, M, J, and I are the total width, mass, spin, and isospin of the resonance, $\beta_{\pi N}$ is its branching ratio to the πN channel, m is the nucleon mass, k_r and q_r are momenta of the real photon and pion at the resonance position in c.m.s.

In the range of Q^2, which we investigate in this paper, there is no information on the helicity amplitudes for the resonances from the third resonance region, and the data [11] do not allow us to extract reliably these amplitudes [except those for $N(1680)F_{15}$] as only part of this region is covered by the data. While we expect small influence of these states on the results for the Roper resonance due to the 200–300 MeV mass gaps, we studied the effect quantitatively using two different ways of estimating the strength of the states from the third resonance region.

(i) By directly including these states in the fit.
(ii) By applying available constraints on their amplitudes. Using symmetry relations within multiplet [70, 1$^-$] given by the single quark transition model [20], we have expressed the transverse amplitudes for the members of this multiplet: $\Delta(1620)S_{31}$, $N(1650)S_{11}$, $N(1675)D_{15}$, $N(1700)D_{13}$, and $\Delta(1700)D_{33}$, through the amplitudes of $N(1520)D_{13}$ and $N(1535)S_{11}$ which are well determined in the analysis. The longitudinal amplitudes of these resonances and the amplitudes of the resonances $\Delta(1600)P_{33}$ and $N(1710)P_{11}$, which have small photocouplings [17] and are not seen in low Q^2 π and 2π electroproduction [14], were assumed to be zero.

The results obtained for $\Delta(1232)P_{33}$, $N(1440)P_{11}$, $N(1520)D_{13}$, and $N(1535)S_{11}$ in the two fits were very close to each other. The amplitudes of the Roper resonance presented below are the average values of the results obtained in these fits. The uncertainties arising from the averaging procedure we will refer to as uncertainties (I). They were included in quadrature into the total model uncertainties of our results.

The background of both approaches contains Born terms corresponding to the s- and u- channel nucleon exchanges and t-channel pion contribution, and depends, therefore, on the proton, neutron, and pion form factors. The background of the UIM contains also the ρ and ω t-channel exchanges [15] and, therefore, the contribution of the form factors $G_{\rho(\omega)\rightarrow\pi\gamma}(Q^2)$. All of these form factors, except the neutron electric and $G_{\rho(\omega)\rightarrow\pi\gamma}(Q^2)$ ones, are known in the region of Q^2 under investigation from existing experimental data. For the proton form factors we used the parametrizations found for the existing data in Ref. [21]. The neutron magnetic form factor and the pion form factor were taken from Refs. [22] and [23–26], respectively. The neutron electric form factor, $G_{E_n}(Q^2)$, is measured up to $Q^2 = 1.45$ GeV^2 [27], and Ref. [27] presents a parametrization for all existing data on $G_{E_n}(Q^2)$ that we used to extrapolate $G_{E_n}(Q^2)$ to $1.7 < Q^2 < 4.2$ GeV^2. In the final results we accounted for a 50%

uncertainty in this extrapolation. There are no measurements of the form factors $G_{\rho(\omega)\to\pi\gamma}(Q^2)$; however, investigations made using both QCD sum rules [28] and quark model [29] predict a Q^2 dependence of $G_{\rho(\omega)\to\pi\gamma}(Q^2)$ close to the dipole form factor $G_d(Q^2) = 1/(1 + \frac{Q^2}{0.71\,\text{GeV}^2})^2$. In our analysis we assumed that $G_{\rho(\omega)\to\pi\gamma}(Q^2) = G_d(Q^2)$, and accounted for a 50% uncertainty in this assumption. All of these uncertainties, including those that arise from the measured proton, neutron, and pion form factors, were added in quadrature and are referred to as model uncertainties (II) in our final results.

The fit to the data was performed for Q^2 bins in the $\vec{e}p \to en\pi^+$ measurements: $Q^2 = 1.72$, 2.05, 2.44, 2.91, 3.48, 4.16 GeV^2 [11]. In this range of Q^2, the available $ep \to ep\pi^0$ data are related mostly to the $\Delta(1232)P_{33}$ resonance region [30–32]. At higher energies there is only small amount of the DESY data [33] (~ 500 data points) for $Q^2 \approx 3$ GeV^2 which have large errors and very limited angular coverage. Our analysis showed that the combined $\vec{e}p \to en\pi^+$ [11] and $ep \to ep\pi^0$ [30–33] data give results that are very close to those obtained from the $\vec{e}p \to en\pi^+$ data [11] alone. For this reason, and also to avoid mixing data sets with different and for the DESY data unknown systematic uncertainties, we present the results for N(1440)P$_{11}$ obtained from the analysis of the $\vec{e}p \to en\pi^+$ data [11] only.

The obtained results for χ^2 are given in Table I. Relatively large values of χ^2 for differential cross sections at $Q^2 = 1.72$, 2.05 GeV^2 are caused by small statistical errors which increase with increasing Q^2. The values of χ^2 for $A_{LT'}$ are somewhat large, however, as can be seen from Fig. 1, the overall description is satisfactory; there are only shortcomings in details.

In Fig. 1, we present the comparison of our results with the experimental data for the lowest Legendre moments of the structure functions at $Q^2 = 2.05$ GeV^2 [11]. Due to interference effects and to the large width of the N(1440)P$_{11}$, this state plays a significant role in the entire W range covered by the data. The Legendre moment $D_0^{T+\epsilon L}$ is related to the $\gamma^*N \to N\pi$ total cross section: $\sigma_{tot} = 4\pi D_0^{T+\epsilon L}$. Being the

$\cos\theta_\pi^*$ independent part of $\sigma_T + \epsilon\sigma_L$, it does not contain interference of different multipole amplitudes and is related to the sum of squares of these amplitudes. The resonance behavior of the multipole amplitudes is revealed in $D_0^{T+\epsilon L}$ in the form of enhancements. Resonance structures related to the resonances $\Delta(1232)P_{33}$ and N(1520)D$_{13}$, N(1535)S$_{11}$ are clearly seen in $D_0^{T+\epsilon L}$. There is a shoulder between the Δ and 1.5 GeV peaks, which is related to the broad Roper resonance. To demonstrate this, we present in Fig. 1 the curves obtained by switching off the N(1440)P$_{11}$ resonance in the final DR results. A fit to the data with the Roper amplitudes put to zero results in $\chi^2 \approx 7$ and gives a dip in $D_0^{T+\epsilon L}$ of the same size as in Fig. 1. This clearly shows that the data can not be explained without Roper resonance.

We now discuss the results for the $\gamma^*p \to$N(1440)P$_{11}$ helicity amplitudes presented in Table II and Fig. 2. The results obtained using DR and UIM are given in Table II separately. It can be seen that they are quite close to each other and give consistent Q^2 behavior of the helicity amplitudes. As the nonresonant background of these approaches is built in conceptually different ways, we conclude that the model uncertainties of the obtained results are relatively small. In Fig. 2 we present average values of the results obtained within the DR and UIM approaches. The uncertainties that originate from this averaging procedure are referred to as model uncertainties (III) in our final results.

Combined with the information obtained from the previous CLAS data at $Q^2 = 0.4$, 0.65 GeV^2 [13,14,31,34–36], and that at $Q^2 = 0$ [17], our results show the following behavior of the transverse helicity amplitude $A_{1/2}$: being large and negative at $Q^2 = 0$, it crosses zero between $Q^2 = 0.4$ and 0.65 GeV^2 and becomes large and positive at $Q^2 \simeq 2$ GeV^2. With increasing Q^2, this amplitude drops smoothly in magnitude. The longitudinal helicity amplitude $S_{1/2}$, which is large and positive at small Q^2, drops smoothly with increasing Q^2.

In Fig. 2, we compare our results with model predictions. These are (i) quark model predictions [1,37–40] where the N(1440)P$_{11}$ is described as the first radial excitation of the $3q$ ground state; (ii) those assuming the N(1440)P$_{11}$ is a hybrid state [6]; and (iii) the results for the Roper resonance treated as a quark core (which is a radial excitation of the $3q$ ground state) dressed by a meson cloud [7,8].

It is known that with increasing Q^2, when the momentum transfer becomes larger than the masses of the constituent quarks, a relativistic treatment of the electroexcitation of the nucleon resonances, which is important already at $Q^2 = 0$, becomes crucial. A consistent way to perform the relativistic treatment of the $\gamma^*N \to N^*$ transitions is to consider them in light-front (LF) dynamics. In Fig. 2 we present the results obtained in the LF quark models [1,37–40]. All LF approaches [1,37–40] give good descriptions of nucleon form factors, however, the predictions for the $\gamma^*N \to$N(1440)P$_{11}$ helicity amplitudes differ significantly. This is caused by the large sensitivity of these amplitudes to the N and N(1440)P$_{11}$ wave functions [40]. The approaches [1,37–40] fail to describe the value of the transverse amplitude $A_{1/2}$ at $Q^2 = 0$. This can be an indication of a large meson cloud contribution to $\gamma^*p \to$N(1440)P$_{11}$, which is expected to be significant at small Q^2. As a confirmation of this assumption, one can

TABLE I. Obtained values of $\chi 2$ for differential cross sections $(\frac{d\sigma}{d\Omega})$ and polarized beam asymmetries ($A_{LT'}$) for $\vec{e}p \to en\pi^+$ data [11].

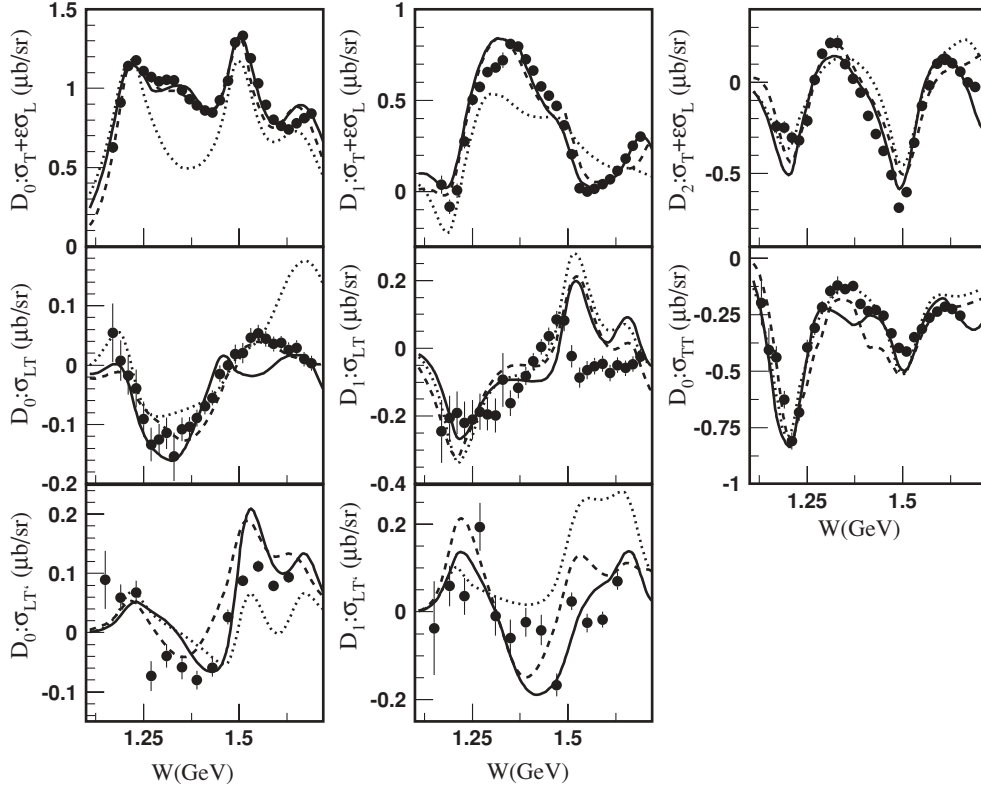| Observable	Q^2 (GeV^2)	Number of data points	$\chi 2$/data DR	UIM
$\frac{d\sigma}{d\Omega}$	1.72	3234	2.3	2.5
	2.05	5123	2.3	2.2
	2.44	5452	1.9	2.0
	2.91	5484	1.9	2.1
	3.48	5482	1.3	1.4
	4.16	5778	1.1	1.1
$A_{LT'}$	1.72	699	2.9	3.0
	2.05	721	3.0	2.9
	2.44	725	3.0	3.0
	2.91	767	2.7	2.7
	3.48	623	2.8	2.7

FIG. 1. Our results for the Legendre moments of the $\vec{e}p \rightarrow en\pi^+$ structure functions in comparison with experimental data [11] for $Q^2 = 2.05$ GeV^2. The solid (dashed) curves correspond to the results obtained using DR (UIM) approach. The dotted curves are obtained by switching off the N(1440)P$_{11}$ resonance in the final DR results.

TABLE II. The $\gamma^* p \rightarrow$ N(1440)P$_{11}$ helicity amplitudes found from the analysis of π^+ electroproduction data [11] using DR and UIM. The first and second uncertainties are, respectively, the statistical uncertainty from the fit and the model uncertainties (I) and (II) added in quadrature.

Q^2	$A_{1/2}$	$S_{1/2}$
(GeV^2)	$(10^{-3}$ GeV$^{-1/2})$	
	DR	
1.72	$72.5 \pm 1.0 \pm 4.3$	$24.8 \pm 1.4 \pm 5.3$
2.05	$72.0 \pm 0.9 \pm 4.2$	$21.0 \pm 1.7 \pm 5.0$
2.44	$50.0 \pm 1.0 \pm 3.2$	$9.3 \pm 1.3 \pm 4.1$
2.91	$37.5 \pm 1.1 \pm 2.8$	$9.8 \pm 2.0 \pm 2.3$
3.48	$29.6 \pm 0.8 \pm 2.7$	$4.2 \pm 2.5 \pm 2.3$
4.16	$19.3 \pm 2.0 \pm 3.9$	$10.8 \pm 2.8 \pm 4.5$
	UIM	
1.72	$58.5 \pm 1.1 \pm 4.2$	$26.9 \pm 1.3 \pm 5.3$
2.05	$62.9 \pm 0.9 \pm 3.3$	$15.5 \pm 1.5 \pm 4.9$
2.44	$56.2 \pm 0.9 \pm 3.2$	$11.8 \pm 1.4 \pm 4.1$
2.91	$42.5 \pm 1.1 \pm 2.8$	$13.8 \pm 2.1 \pm 2.3$
3.48	$32.6 \pm 0.9 \pm 2.6$	$14.1 \pm 2.4 \pm 2.0$
4.16	$23.1 \pm 2.2 \pm 4.8$	$17.5 \pm 2.6 \pm 5.5$

consider the results of Refs. [7,8] where this contribution is taken into account, and a good description of the helicity amplitudes is obtained at small Q^2.

In spite of the differences, all LF predictions for the $\gamma^* p \rightarrow$ N(1440)P$_{11}$ helicity amplitudes have common features that agree with the results extracted from the experimental data: (i) the sign of the transverse amplitude $A_{1/2}$ at $Q^2 = 0$ is negative, (ii) the sign of the longitudinal amplitude $S_{1/2}$ is positive, (iii) all LF approaches predict the sign change of the transverse amplitude $A_{1/2}$ at small Q^2. We take this qualitative agreement as evidence in favor of the N(1440)P$_{11}$ resonance as a radial excitation of the $3q$ ground state. Final confirmation of this conclusion requires a complete simultaneous description of the nucleon form factors and the $\gamma^* p \rightarrow$ N(1440)P$_{11}$ amplitudes. This will allow us to find the magnitude of the meson cloud contribution, and to better specify the N and N(1440)P$_{11}$ wave functions. To achieve a satisfactory description at large Q^2, it may be necessary to take into account quark form factors, as well as other effects, such as the quark mass dependence on the momentum transfer.

The results of Refs. [5,6], where N(1440)P$_{11}$ is treated as a hybrid state, are obtained via non-relativistic calculations. Nevertheless the suppression of the longitudinal amplitude $S_{1/2}$ has a physical origin, which makes this result practically independent of relativistic effects. The predicted suppression of the longitudinal amplitude $S_{1/2}$ strongly disagrees with the experimental results.

In summary, for the first time the transverse and longitudinal helicity amplitudes of the $\gamma^* p \rightarrow$ N(1440)P$_{11}$ transition are extracted from experimental data at high Q^2. The results are obtained from differential cross sections and longitudinally
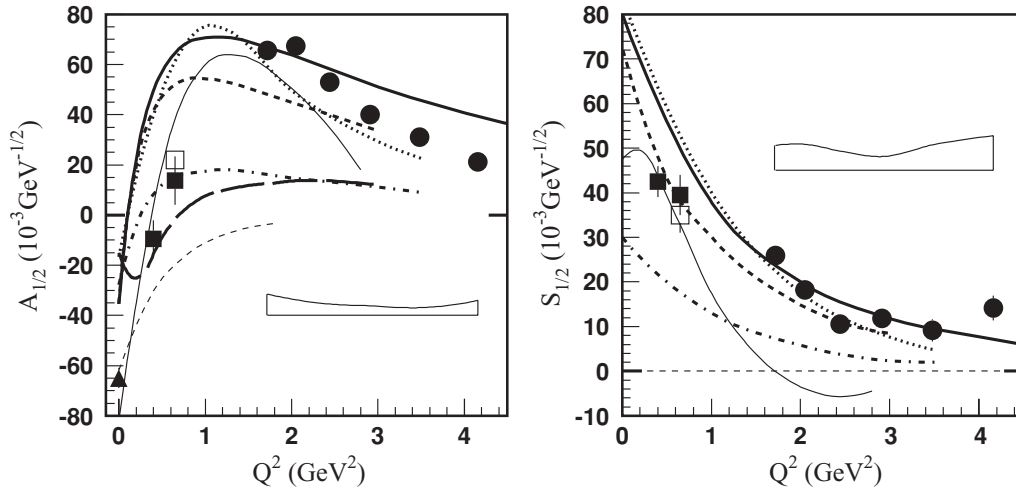
FIG. 2. Helicity amplitudes for the $\gamma^* p \to$ N(1440)P$_{11}$ transition. The full circles are our results obtained from the analysis of π^+ electroproduction data [11]. The bands present the model uncertainties (I,II,III) added in quadrature; see text. The full boxes are the results obtained from CLAS data [13,31,34–36]; open boxes present the results of the combined analysis of CLAS single π and 2π electroproduction data [14]. The full triangle at $Q^2 = 0$ is the RPP estimate [17]. The thick curves correspond to the light-front relativistic quark models: dotted, dashed, dash-dotted, long-dashed, and solid curves are from Refs. [1,37–40], respectively. The thin solid curves are the predictions obtained for the Roper resonance treated as a quark core dressed by a meson cloud [7,8]. The thin dashed curves are obtained assuming that N(1440)P$_{11}$ is a q^3G hybrid state [6].

polarized beam asymmetries for π^+ electroproduction on protons at $W = 1.15 - 1.69$ GeV [11]. The data were analyzed using two conceptually different approaches, DR and UIM, which give consistent results for Q^2 behavior of the extracted helicity amplitudes.

Comparison with quark model predictions provides strong evidence in favor of N(1440)P$_{11}$ as a first radial excitation of the $3q$ ground state.

The results for the longitudinal helicity amplitude confirm our conclusion made from the previous analysis of CLAS $\vec{e}p \to ep\pi^0, en\pi^+$ data for $Q^2 < 1$ GeV^2 [13] that the presentation of the Roper resonance as a q^3G hybrid state is ruled out.

[1] S. Capstick and B. D. Keister, Phys. Rev. D **51**, 3598 (1995).

[2] S. Capstick and N. Isgur, Phys. Rev. D **34**, 2809 (1986).

[3] J.-M. Richard, Phys. Rep. **212**, 1 (1992).

[4] L. Ya. Glozman and D. O. Riska, Phys. Rep. **268**, 263 (1996).

[5] Z. P. Li, Phys. Rev. D **44**, 2841 (1991).

[6] Z. P. Li, V. Burkert, and Zh. Li, Phys. Rev. D **46**, 70 (1992).

[7] F. Cano, P. González, S. Noguera, and B. Desplanques, Nucl. Phys. **A603**, 257 (1996).

[8] F. Cano and P. González, Phys. Lett. **B431**, 270 (1998).

[9] O. Kreil, C. Hanhart, C. Krewald, and J. Speth, Phys. Rev. C **62**, 025207 (2000).

[10] M. Dillig and M. Schott, Phys. Rev. C **75**, 067001 (2007).

[11] K. Park *et al.* (CLAS Collaboration), Phys. Rev. C **77**, 015208 (2008).

[12] I. G. Aznauryan, Phys. Rev. C **67**, 015209 (2003).

[13] I. G. Aznauryan, V. D. Burkert, H. Egiyan, K. Joo, R. Minehart, and L. C. Smith, Phys. Rev. C **71**, 015201 (2005).

[14] I. G. Aznauryan, V. D. Burkert, G. V. Fedotov, B. S. Ishkhanov, and V. I. Mokeev, Phys. Rev. C **72**, 045201 (2005).

[15] D. Drechsel, O. Hanstein, S. Kamalov, and L. Tiator, Nucl. Phys. **A645**, 145 (1999).

[16] D. Drechsel, S. Kamalov, and L. Tiator, Eur. Phys. J. A **34**, 69 (2007).

[17] W.-M. Yao *et al.* (Particle Data Group), J. Phys. G **33**, 1 (2006).

[18] R. A. Arndt, R. L. Workman, Zh. Li, and L. D. Roper, Phys. Rev. C **42**, 1864 (1990).

[19] L. Tiator, D. Drechsel, S. Kamalov, and S. N. Yang, PiN Newslett. **16**, 41 (2002).

[20] V. D. Burkert, R. Devita, M. Battaglieri, M. Ripani, and V. Mokeev, Phys. Rev. C **67**, 035204 (2003).

[21] J. Arrington, W. Melnitchouk, and J. A. Tjon, Phys. Rev. C **76**, 035205 (2007).

[22] W. K. Brooks *et al.*, Nucl. Phys. **A755**, 261 (2005).

[23] C. J. Bebek *et al.*, Phys. Rev. D **13**, 25 (1976).

[24] C. J. Bebek *et al.*, Phys. Rev. D **17**, 1693 (1978).

[25] T. Horn *et al.*, Phys. Rev. Lett. **97**, 192001 (2006).

[26] V. Tadevosyan *et al.*, Phys. Rev. C **75**, 055205 (2007).

[27] R. Madey *et al.*, Phys. Rev. Lett. **91**, 122002 (2003).

[28] V. Eletski and Ya. Kogan, Yad. Fiz. **39**, 138 (1984).

[29] I. Aznauryan and K. Oganessyan, Phys. Lett. **B249**, 309 (1990).

[30] V. V. Frolov *et al.*, Phys. Rev. Lett. **82**, 45 (1999).

[31] K. Joo *et al.* (CLAS Collaboration), Phys. Rev. Lett. **88**, 122001 (2002).

[32] M. Ungaro *et al.* (CLAS Collaboration), Phys. Rev. Lett. **97**, 112003 (2006).

[33] R. Haidan, Ph.D. thesis, University of Hamburg, Hamburg, 1979.

[34] K. Joo *et al.* (CLAS Collaboration), Phys. Rev. C **68**, 032201(R) (2003).

[35] K. Joo *et al.* (CLAS Collaboration), Phys. Rev. C **70**, 042201(R) (2004).

[36] H. Egiyan *et al.* (CLAS Collaboration), Phys. Rev. C **73**, 025204 (2006).

[37] H. J. Weber, Phys. Rev. C **41**, 2783 (1990).

[38] F. Cardarelli, E. Pace, G. Salme, and S. Simula, Phys. Lett. **B397**, 13 (1997).

[39] B. Juliá-Díaz, D. O. Riska, and F. Coester, Phys. Rev. C **69**, 035212 (2004).

[40] I. G. Aznauryan, Phys. Rev. C **76**, 025212 (2007).